nature neuroscience

Piezo2 is the principal mechanotransduction channel for proprioception

Seung-Hyun Woo[1], Viktor Lukacs[1], Joriene C de Nooij[2,3], Dasha Zaytseva[4], Connor R Criddle[4], Allain Francisco[1], Thomas M Jessell[2,3], Katherine A Wilkinson[4] & Ardem Patapoutian[1]

Proprioception, the perception of body and limb position, is mediated by proprioceptors, specialized mechanosensory neurons that convey information about the stretch and tension experienced by muscles, tendons, skin and joints. In mammals, the molecular identity of the stretch-sensitive channel that mediates proprioception is unknown. We found that the mechanically activated nonselective cation channel Piezo2 was expressed in sensory endings of proprioceptors innervating muscle spindles and Golgi tendon organs in mice. Two independent mouse lines that lack Piezo2 in proprioceptive neurons showed severely uncoordinated body movements and abnormal limb positions. Moreover, the mechanosensitivity of parvalbumin-expressing neurons that predominantly mark proprioceptors was dependent on Piezo2 expression *in vitro*, and the stretch-induced firing of proprioceptors in muscle-nerve recordings was markedly reduced in Piezo2-deficient mice. Together, our results indicate that Piezo2 is the major mechanotransducer of mammalian proprioceptors.

Proprioception is the sense of body and limb position and is transduced by proprioceptive sensory neurons[1,2]. The information encoded by proprioceptors contributes to both unconscious (for example, knee jerk reflex) and conscious (for example, the ability to touch one's nose with eyes closed) sensations and is required for basic motor functions such as standing and walking[3]. In mammals, proprioceptors represent anatomically distinct sensory neurons that have cell bodies in dorsal root ganglia (DRG) and innervate two distinct mechanoreceptors in skeletal muscles: muscle spindles (MSs) and Golgi tendon organs (GTOs)[2,4]. MS afferents innervate intrafusal muscle fibers and detect changes in muscle length, whereas GTO afferents innervate the tendon organs at the myo-tendinous junction and respond to changes in muscle tone[2,4].

The molecular mechanism(s) underlying proprioception has been a long-standing question. In particular, the identification of ion channel(s) that are thought to transduce mechanical strain experienced by muscles and joints into electrical signals has been a major topic of research, and study has focused on the transient receptor potential (TRP) and Degenerin/Epithelial Na^+ Channel (DEG/ENaC) families[4]. In *Drosophila*, the TRPN/NompC channel is expressed in both bipolar dendrite (bd) and class I dendritic arborization (da) proprioceptive neurons, and is required for proper larval crawling and behavioral coordination in adult flies[5,6]. In *C. elegans*, *trp-4* (a TRPN/NompC homolog) and *unc-8* (a DEG/ENaC family member) have been implicated in proprioception, as mutations in these genes cause impaired movement in worms[7,8]. More recently, Piezo has also been shown to mediate stretch-activated firing of larval *Drosophila* dorsal bipolar dendritic (dbd) neurons[9].

In mammals, however, the molecular mechanism underlying proprioception has remained largely elusive. Previous studies have suggested that mechanically activated (MA) currents in mammalian proprioceptive neurons are largely mediated by Na^+ ions, with Ca^{2+} ions having a minor role[10]. Consistent with this observation, ENaC proteins are expressed in rat MSs[11]. However, no strong evidence has been provided for ENaC proteins in mammalian proprioception[4,11].

Piezo family members are nonselective cation channels with diverse roles in mechanotransduction and volume signaling[12–18]. In mice, Piezo1 has a critical role in vascular remodeling and red blood cell volume regulation[13,15,18], whereas Piezo2 is expressed in sensory neurons and functions as the mechanotransducer for low-threshold mechanoreceptors in murine skin[14,16,17]. We found that parvalbumin (Pvalb)-expressing sensory neurons, which correspond primarily to proprioceptors[19], express nonselective MA cationic currents whose biophysical properties are consistent with Piezo2 channels[12,16]. Based on these observations, we explored whether Piezo2 is involved in mammalian proprioception.

RESULTS

MA cation channel Piezo2 is expressed in proprioceptors

MA currents in proprioceptive neurons are thought to be mediated by Na^+ ions, with Ca^{2+} ions having a minor role[4,10]. This assertion is based on stretch-induced extracellular voltage recordings of MS afferents[10]. The voltage changes recorded in such preparations are a result of the coordinated opening of multiple ion channels. To determine the ion selectivity of the mechanotransducer channel itself, we performed electrophysiological recordings in proprioceptors *in vitro*[16,20].

[1]Howard Hughes Medical Institute, Molecular and Cellular Neuroscience, Dorris Neuroscience Center, The Scripps Research Institute, La Jolla, California, USA. [2]Howard Hughes Medical Institute, Department of Neuroscience, Columbia University, New York, New York, USA. [3]Howard Hughes Medical Institute, Department of Biochemistry and Molecular Biophysics, Columbia University, New York, New York, USA. [4]Department of Biological Sciences, San José State University, San Jose, California, USA. Correspondence should be addressed to A.P. (ardem@scripps.edu).

Received 14 July; accepted 13 October; published online 9 November 2015; doi:10.1038/nn.4162

To label proprioceptive neurons, we crossed *Pvalb-Cre* mice[21], which express Cre recombinase in all proprioceptors and a few rapidly adapting low-threshold cutaneous mechanoreceptors[19], with *Ai9* tdTomato reporter mice[22] (**Supplementary Fig. 1a**). DRG neurons from *Pvalb-Cre; Ai9* mice were isolated, and tdTomato$^+$ neurons were visually selected and subjected to whole-cell patch-clamp recordings *in vitro* (**Fig. 1a**). Although physiological mechanotransduction occurs at the nerve terminals, many MA channels are also expressed in, and can be recorded from, DRG cell bodies[20]. Mechanical stimuli were applied to tdTomato$^+$ neurons using a blunt-end glass probe (**Fig. 1b**)[12,16]. All tdTomato$^+$ neurons responded to this mechanical stimulus: 92% (23 of 25) of the neurons displayed rapidly adapting (RA) currents (inactivation time constant $\tau = 5.6 \pm 0.33$ ms) and 8% (2 of 25) exhibited intermediately adapting (IA) currents ($\tau = 15.56$ and 31.67 ms) (**Fig. 1b**). To determine ionic selectivity, we performed current-voltage (I-V) relationship measurements. The RA currents, which form the vast majority of MA responses, had a reversal potential (E_{rev}) of $+13.55 \pm 0.73$ mV (**Fig. 1c**). These E_{rev} values are inconsistent with Na$^+$-selective channels, as the theoretical E_{rev} for Na$^+$ in our conditions is +64 mV. In addition, we found that application of 100 µM amiloride (an inhibitor of DEG/ENaC Na$^+$ channels) to these cells via bath perfusion had no effect on either current amplitude or I-V relationship of these traces ($E_{rev} = +11.72 \pm 0.91$ mV). These two observations, E_{rev} values close to 0 mV and the lack of inhibition by amiloride, suggest that nonselective, amiloride-insensitive channels mediate the majority of MA currents in Pvalb$^+$ neurons. One of the two cells displaying IA currents reversed at +0.42 mV (**Supplementary Fig. 1b**). As a result of the low frequency of IA current observations, our conclusions about this cell population are limited, and we cannot determine whether they were expressed in proprioceptors or the aforementioned Pvalb$^+$ cutaneous mechanoreceptors[19]. Nevertheless, the observed E_{rev} value was also inconsistent with this current being mediated by Na$^+$-selective channels.

The inactivation kinetics, reversal potential and voltage dependence of the RA currents that we observed in Pvalb$^+$ neurons resemble those of Piezo2 expressed in heterologous systems (for example, Piezo2 in HEK293T cells, $\tau = 7.3 \pm 0.7$ ms, $E_{rev} = +8.7 \pm 1.5$ mV)[12]. Piezo2 is a nonselective MA cation channel present in the sensory endings of low-threshold cutaneous mechanoreceptors[16]. To address whether Piezo2 channels could underlie the nonselective RA current that we observed in proprioceptors, we first asked whether Piezo2 is expressed in these sensory neurons. To assess Piezo2 expression in proprioceptors, we used the previously reported *Piezo2^{GFP}* reporter line, in which *GFP* is fused to the last coding exon of *Piezo2* and is expressed as a Piezo2-GFP fusion protein under the endogenous *Piezo2* promoter[17]. We examined *Piezo2^{GFP}* lumbar DRG by immunostaining for GFP and Pvalb and found that 81% of Pvalb$^+$

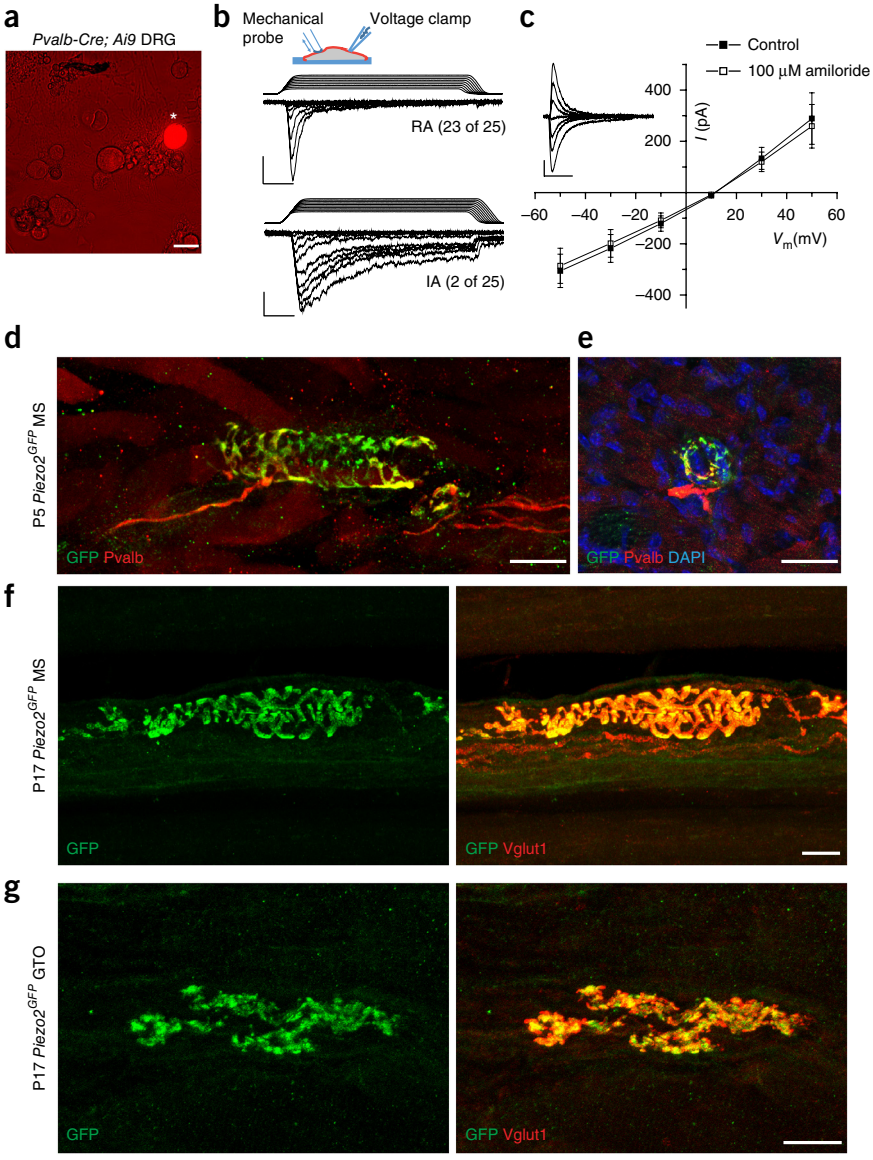

Figure 1 Characterization of mechanically activated currents and Piezo2 expression in proprioceptive neurons. (**a**) tdTomato$^+$ neuron (asterisk) in isolated DRG cultures from adult *Pvalb-Cre; Ai9* mice. (**b**) Whole-cell voltage-clamp recordings from tdTomato$^+$ DRG neurons using mechanical stimuli by displacement of a blunt glass probe in 1-µm increments. Example traces of tdTomato$^+$ DRG neurons responding with RA ($\tau_{inact} < 10$ ms) and IA (10 ms $< \tau_{inact} <$ 30 ms) MA currents from *Pvalb-Cre; Ai9* mice are shown ($n = 25$ neurons total). Inset depicts experimental setting; ramp-and-hold traces on top of current recordings show displacement of glass probe. Vertical scale bars represent 100 pA. Horizontal scale bars represent 25 ms. Holding potential, −60 mV. (**c**) I-V relationship of RA responses at 4–5 µm past mechanical threshold before (closed squares) and after (open squares) the application of 100 µM amiloride ($n = 11$ neurons in each group). Representative background-subtracted control trace shown in inset. Vertical scale bar represents 200 pA. Horizontal scale bar represents 25 ms. (**d**) Immunofluorescence for GFP and Pvalb in MS from P5 *Piezo2^{GFP}* hind leg muscle. (**e**) Immunofluorescence for GFP and Pvalb in MS in a transverse section of P5 *Piezo2^{GFP}* intercostal muscle. (**f**,**g**) Immunofluorescence for GFP and Vglut1 in MS (**f**) and in GTO (**g**) from P17 *Piezo2^{GFP}* hind leg muscle. Scale bars represent 30 µm (**a**) and 20 µm (**d**–**g**).

neurons (191 of 236) expressed GFP (**Supplementary Fig. 2a**). Next, we examined Piezo2 expression in proprioceptor muscle endings, where mechanotransduction initiates. In postnatal day 5 (P5) *Piezo2*^{GFP} hind leg muscles, immunofluorescence for GFP and Pvalb colocalized in every MS sensory ending that we observed (13 GFP$^+$ Pvalb$^+$ MSs of 13 total; **Fig. 1d**), but not in MS intrafusal muscle fibers (**Fig. 1e**). Furthermore, we examined P17 *Piezo2*^{GFP} leg muscles by immunostaining for GFP and Vglut1 (a marker of MS and GTO afferent endings) and detected GFP and Vglut1 in all of the annulospiral endings of both group Ia and group II MS afferents, as well as in every GTO afferent endings encountered (21 GFP$^+$ Vglut1$^+$ MSs of 21 total; 11 GFP$^+$ Vglut1$^+$ GTOs of 11 total; **Fig. 1f**,**g** and **Supplementary Fig. 2b**,**c**). These data suggest that Piezo2 is expressed in all types of proprioceptive peripheral endings.

Piezo2 is required for proprioception in mice

Previously, we found that Piezo2 ablation in sensory neurons of adult mice via the *Advillin-CreER*^{T2} driver caused a severe deficit in cutaneous light-touch sensation[16]. In addition, these mice displayed an unstable gait, but did not exhibit a complete proprioceptive deficit (for example, severely abnormal limb positioning). We reasoned that the proprioceptive behavioral deficits might be more severe if the mice were to lose proprioception from birth rather than during adulthood, after they have learned to walk. Alternatively, given that *Advillin-CreER*^{T2} marks 87% of spinal sensory neurons[16], it is possible that the *Advillin-CreER*^{T2}–driven Piezo2 deletion does not represent a complete ablation of Piezo2 in proprioceptors. To test more definitively whether Piezo2 is involved in proprioception, we used two alternative Cre lines that target proprioceptive neurons during development: *Pvalb-Cre*[21] and *HoxB8-Cre*[23]. As described above, *Pvalb-Cre* targets all proprioceptive neurons and a subset of cutaneous mechanoreceptors[19], whereas *HoxB8-Cre* targets broader neuronal populations in caudal DRG, including the proprioceptors[23] (**Supplementary Fig. 3**).

We generated two tissue-specific Piezo2 conditional knockout (cKO) mouse lines by crossing the *Pvalb-Cre* and *HoxB8-Cre* lines to *Piezo2*$^{fl/fl}$ mice[17] (**Supplementary Figs. 4a**,**b** and **5a**,**b**). Both *Pvalb-Cre; Piezo2*^{cKO} and *HoxB8-Cre; Piezo2*^{cKO} mice were born at the expected Mendelian ratio and were indistinguishable from their control littermates in body size or body movement shortly after birth. Notably, postnatal Piezo2 cKO mice (as early as P7) displayed severely impaired limb coordination compared with their control littermates (**Fig. 2a**,**b** and **Supplementary Videos 1–4**). Typically, wild-type (WT) mice stretch out their limbs when lifted by their tails (**Fig. 2a**,**b**). In the case of *Pvalb-Cre; Piezo2*^{cKO} and *HoxB8-Cre; Piezo2*^{cKO} mice, they clenched their toes and awkwardly positioned their limbs so that their limbs were either completely folded or pointing to atypical directions (**Fig. 2a**,**b**).

Consistent with the aforementioned caudal bias in the HoxB8-Cre activity in DRG, we found that only hind limbs were affected in

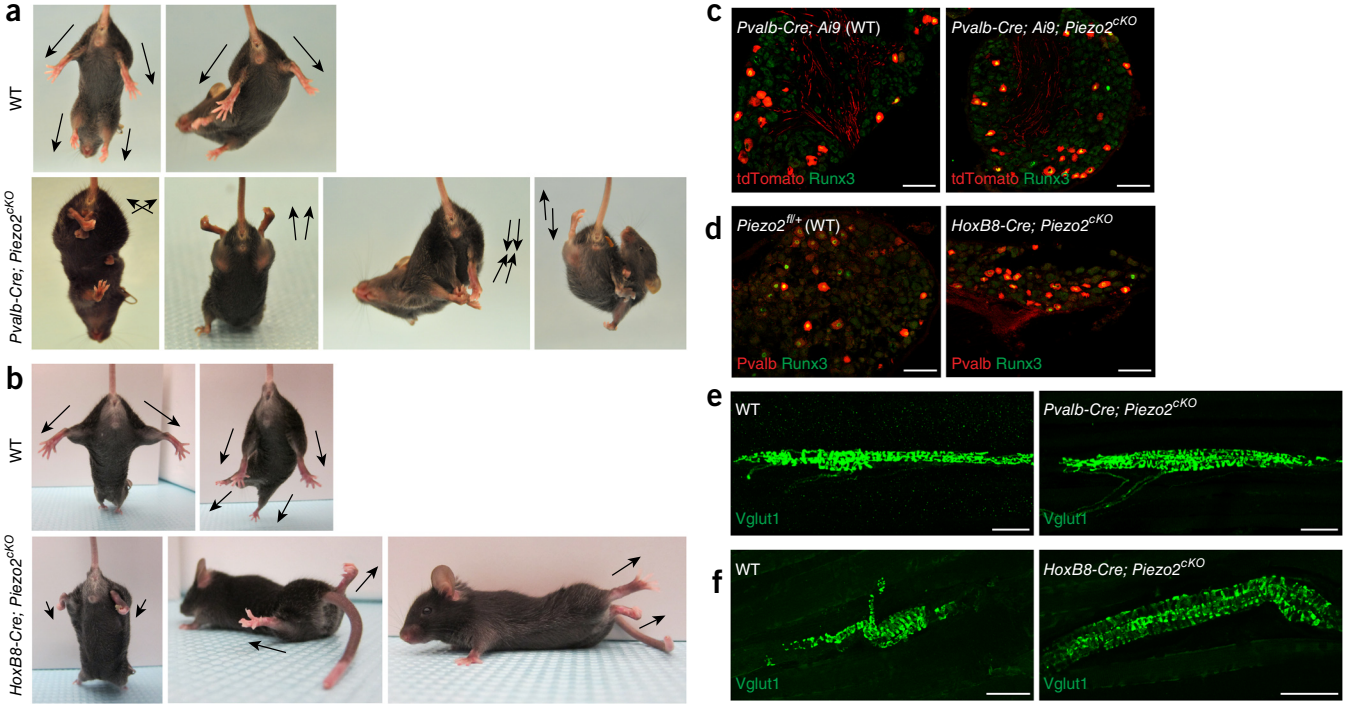

Figure 2 Characterization of two tissue-specific Piezo2 conditional knockout mice. (**a**,**b**) Representative images showing limb positions of 4–5-week-old WT littermate and *Pvalb-Cre; Piezo2*^{cKO} mice (**a**) and WT littermate and *HoxB8-Cre; Piezo2*^{cKO} mice (**b**). Arrows mark the direction of the limbs. (**c**) Runx3 immunostaining with tdTomato epifluorescence in lumbar DRG from 4–5-week-old *Pvalb-Cre; Ai9* (WT, left) and *Pvalb-Cre; Ai9; Piezo2*^{cKO} (right) mice (WT: tdTomato$^+$ neurons, 15.4%, 154 of 1,003; tdTomato$^+$ Runx3$^+$ neurons, 6.8%, 68 of 1,003; cKO: tdTomato$^+$ neurons, 15.4%, 204 of 1,327; tdTomato$^+$ Runx3$^+$ neurons, 8.7%, 116 of 1,327). (**d**) Runx3 and Pvalb immunostaining in lumbar DRG from 4–5-week-old WT (left) and *HoxB8-Cre; Piezo2*^{cKO} (right) mice (WT: Pvalb$^+$ neurons, 8.5%, 87 of 1,029; Pvalb$^+$Runx3$^+$ neurons, 6.2%, 64 of 1,029; cKO: Pvalb$^+$ neurons, 8.8%, 83 of 938; Pvalb$^+$Runx3$^+$ neurons, 4.6%, 43 of 938). Note that we detected a higher percentage of Pvalb$^+$ neurons in the *Pvalb-Cre; Ai9* line (15.4%) than in the *HoxB8-Cre* line (8.5%). tdTomato epifluorescence was very strong compared with Pvalb immunostaining in adult DRG; thus, a difference in the detection method could explain the higher percentage of Pvalb$^+$ neurons in the *Pvalb-Cre; Ai9* line. (**e**,**f**) Vglut1 immunostaining in MS endings of 4–5-week-old WT littermate and *Pvalb-Cre; Piezo2*^{cKO} hind leg muscles (**e**) and WT littermate and *HoxB8-Cre; Piezo2*^{cKO} hind leg muscles (**f**). Scale bars represent 100 μm (**c**,**d**) and 50 μm (**e**,**f**).

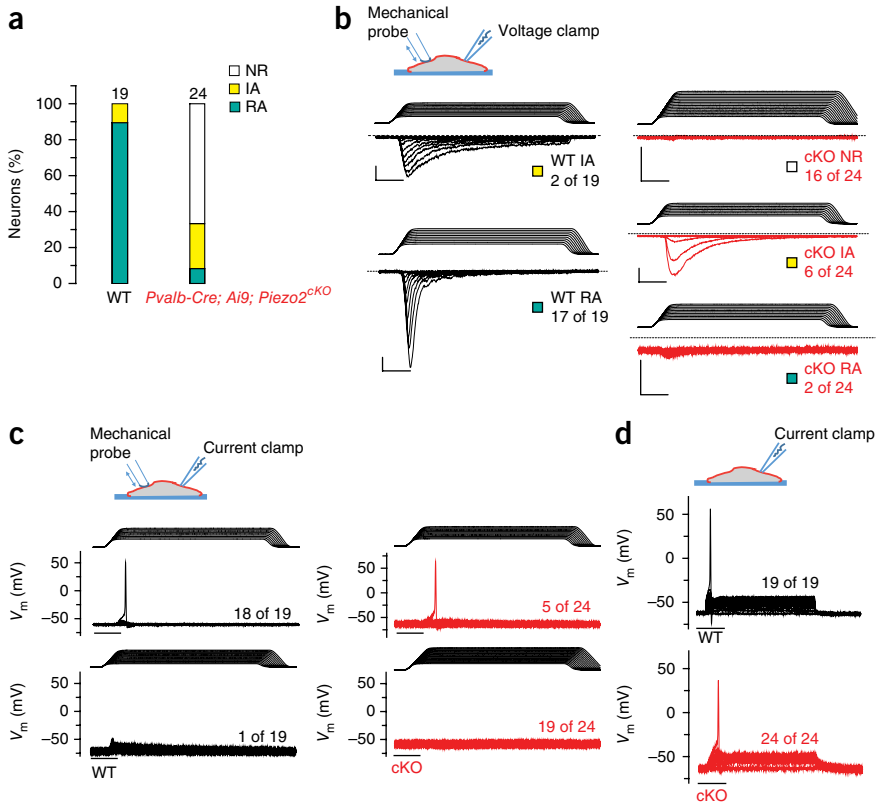

Figure 3 Characterization of MA currents in proprioceptive neurons of Piezo2-deficient mice. Whole-cell patch-clamp recordings were conducted using mechanical stimulation with a blunt-end glass probe in 1-μm increments. (**a**) The proportion of tdTomato+ DRG neurons responding with RA (τ_{inact} < 10 ms) and IA (10 ms < τ_{inact} < 30 ms) MA currents from 4–6-week-old *Pvalb-Cre; Ai9* (WT) and *Pvalb-Cre; Ai9; Piezo2^{cKO}* mice in voltage-clamp experiments. NR, non-responsive to mechanical displacements. (**b**) Example traces of mechanically induced currents in WT (black traces) and cKO (red traces) tdTomato+ neurons. Holding potential, −60 mV. (**c**) Current-clamp recordings of WT (black traces) and cKO (red traces) tdTomato+ neurons with mechanical stimulation. (**d**) Current-clamp recordings of WT (black traces) and cKO tdTomato+ neurons (red traces). Depolarizing currents were injected in 50-pA increments from a holding current of 0 pA. All vertical scale bars represent 200 pA and all horizontal scale bars represent 25 ms. Numbers adjacent to traces indicate the number of neurons represented by the trace of the total number of neurons tested.

HoxB8-Cre; Piezo2^{cKO} mice, whereas all four limbs showed impaired coordination in *Pvalb-Cre; Piezo2^{cKO}* mice (**Supplementary Fig. 3a**,**b**). *Pvalb-Cre; Piezo2^{cKO}* mice stumbled while walking, and their limbs appeared to be stiff in general (**Supplementary Videos 1** and **2**). These phenotypes markedly resembled the walking pattern of *P^{kill}* mice, in which all proprioceptive afferents are eliminated by Diphtheria toxin A induction[3,24]. *HoxB8-Cre; Piezo2^{cKO}* mice displayed more peculiar hind limb coordination defects: consistently raising their hind limbs and dragging their body with their forelimbs (**Supplementary Videos 3** and **4**). This increased severity in phenotype could potentially be a result of broader Piezo2 deletion in DRG neurons compared with the Pvalb+ neurons (**Supplementary Figs. 1a** and **3a**)[16]. Despite their impaired body coordination, both lines of Piezo2 cKO mice were able to eat, drink and groom similar to WT littermates, and we observed no substantial difference in their body weight (data not shown). Piezo2 expression was not observed in cerebellum, motor neurons and interneurons, or skeletal muscle (**Fig. 1d**–**g**, **Supplementary Fig. 2c** and data not shown); thus, Piezo2 cKO behavioral phenotypes are likely to be caused by Piezo2 ablation in proprioceptive sensory neurons.

We next tested whether Piezo2 ablation affected the number of proprioceptive neurons to ensure that impaired proprioception in the two Piezo2 cKO lines was not a result of anatomical deficits. We labeled and quantified the number of proprioceptors by immunofluorescence for Pvalb (or tdTomato) and Runx3 in lumbar DRG of *Pvalb-Cre; Ai9; Piezo2^{cKO}* and *HoxB8-Cre; Piezo2^{cKO}* mice[19]. For both Piezo2 cKO lines, the total number of proprioceptors was comparable to their WT controls (**Fig. 2c**,**d**). We also examined proprioceptor sensory endings in hind leg muscles of Piezo2 cKO lines by Vglut1 immunostaining (**Fig. 2e**,**f**)[19,25], and a comparable number of MS endings was observed between *Pvalb-Cre; Piezo2^{cKO}* and WT littermates (**Supplementary Fig. 4c**). MS endings in Piezo2 cKO muscles generally looked healthy and formed complex annulospiral endings similar to WT muscles for both Piezo2 cKO lines (**Fig. 2e**,**f**), although we occasionally encountered less organized MS endings in cKO muscles (**Supplementary Fig. 4d**). Moreover, central projections of proprioceptors looked similar between Piezo2 cKO mice and their control littermates (**Supplementary Figs. 4e** and **5c**)[19,25]. Taken together, both *Pvalb-Cre; Piezo2^{cKO}* and *HoxB8-Cre; Piezo2^{cKO}* mice exhibit severe proprioceptive deficits in the absence of overt quantitative and structural changes in proprioceptors.

Piezo2 mediates RA MA currents in proprioceptors *in vitro*

Next, we asked whether Piezo2 is required for proprioceptor mechanotransduction. To address this, we performed whole-cell patch-clamp recordings in tdTomato+ neurons isolated from *Pvalb-Cre; Ai9; Piezo2^{cKO}* and *Pvalb-Cre; Ai9* WT DRG (**Supplementary Table 1**). Consistent with our earlier experiments (**Fig. 1b**), all WT neurons responded to mechanical stimulation, with the majority of the responses (89.5%) displaying RA characteristics (τ = 5.89 ± 0.47). In contrast, RA currents were observed in only 8.3% (2 of 24) of Piezo2-deficient tdTomato+ neurons (**Fig. 3a**,**b**). One of the two residual RA currents exhibited currents comparable to those of WT neurons (**Supplementary Fig. 6a**), whereas the other RA response was small in amplitude (**Fig. 3b** and **Supplementary Fig. 6a**). These remaining RA currents in tdTomato+ cKO neurons might be a result of incomplete Piezo2 deletion, as we observed a similar percentage (11.2%) of Pvalb+ neurons with intact *Piezo2* in *Pvalb-Cre; Piezo2^{cKO}* DRG (**Supplementary Fig. 4b**). In contrast, the percentage of IA current responses increased slightly in the *Pvalb-Cre; Ai9; Piezo2^{cKO}* neurons (**Fig. 3a**,**b** and **Supplementary Fig. 6b**). This suggests that the IA currents are not mediated by Piezo2 and might indicate a possible compensatory increase in other MA channels in the absence of Piezo2.

The presence of MA currents detectable in a voltage-clamp setting does not address the issue of biological relevance of these currents to neuronal excitation. We therefore used current-clamp recordings to address whether mechanical stimulation of the soma could elicit

action potentials in WT and Piezo2-deficient tdTomato$^+$ neurons (**Fig. 3c**). In WT neurons, action potentials were evoked by mechanical stimulation in 94.7% of the cases, as compared with only 20.8% in Piezo2 cKO neurons. The difference in mechanically induced action potential firing was not a result of a deficiency of excitability in Piezo2 cKO neurons, as action potentials could be elicited in all WT and Piezo2 cKO neurons by current injection (**Fig. 3d**). Notably, although the resting potential and voltage threshold for action potentials were

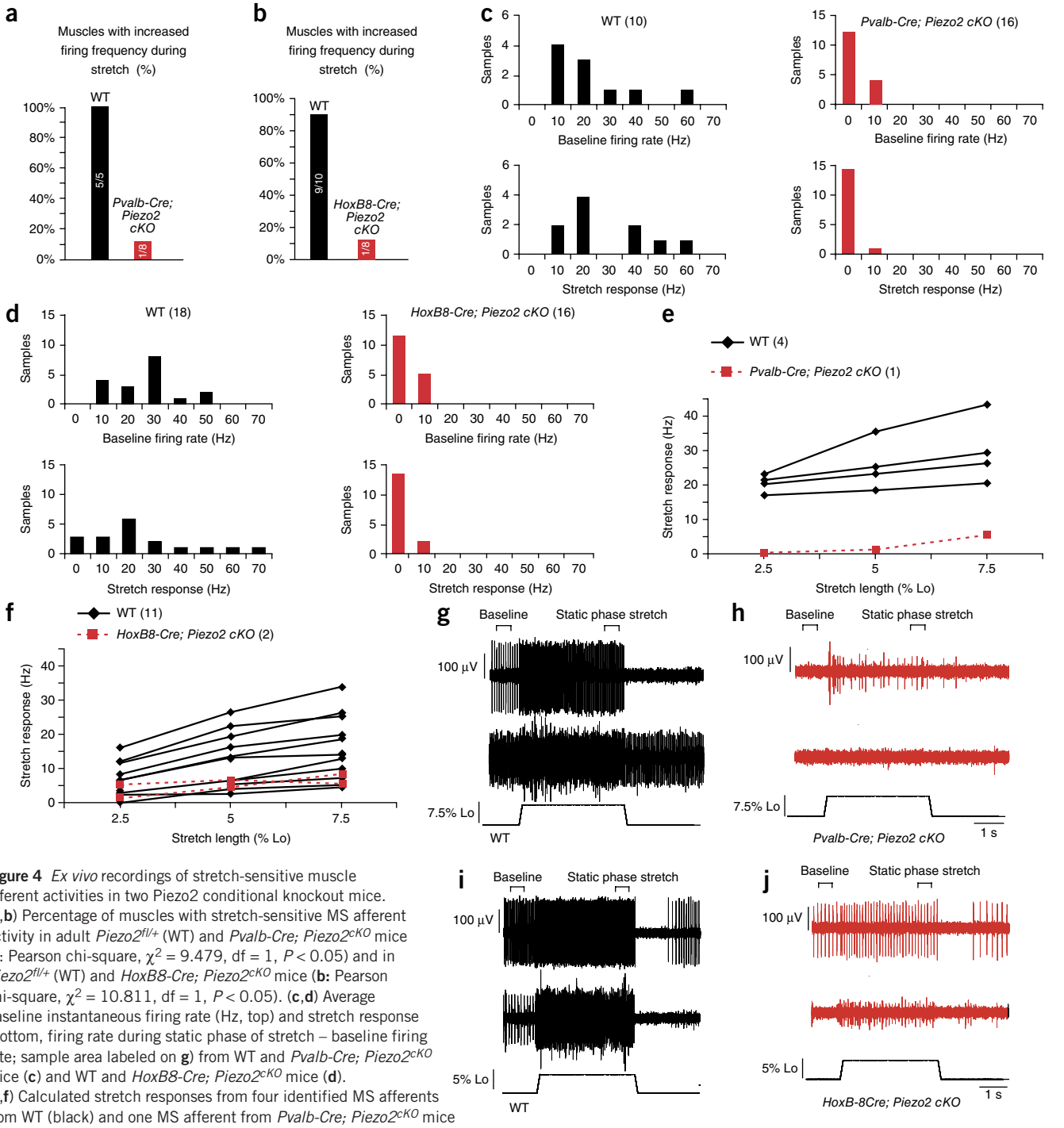

Figure 4 *Ex vivo* recordings of stretch-sensitive muscle afferent activities in two Piezo2 conditional knockout mice. (**a**,**b**) Percentage of muscles with stretch-sensitive MS afferent activity in adult *Piezo2*$^{fl/+}$ (WT) and *Pvalb-Cre; Piezo2*^{cKO} mice (**a**: Pearson chi-square, $\chi^2 = 9.479$, df = 1, $P < 0.05$) and in *Piezo2*$^{fl/+}$ (WT) and *HoxB8-Cre; Piezo2*^{cKO} mice (**b:** Pearson chi-square, $\chi^2 = 10.811$, df = 1, $P < 0.05$). (**c**,**d**) Average baseline instantaneous firing rate (Hz, top) and stretch response (bottom, firing rate during static phase of stretch – baseline firing rate; sample area labeled on **g**) from WT and *Pvalb-Cre; Piezo2*^{cKO} mice (**c**) and WT and *HoxB8-Cre; Piezo2*^{cKO} mice (**d**). (**e**,**f**) Calculated stretch responses from four identified MS afferents from WT (black) and one MS afferent from *Pvalb-Cre; Piezo2*^{cKO} mice (red) (**e**) and from 11 identified MS afferents from WT (black) and two MS afferents from *HoxB8-Cre; Piezo2*^{cKO} mice (red) (**f**). Stretch responses were calculated by subtracting baseline instantaneous firing frequency (Hz) from instantaneous firing frequency during static phase of stretch. (**g**) Two representative responses to stretch from WT muscles (control littermates of *Pvalb-Cre; Piezo2*^{cKO} mice). Top trace includes a single identified MS afferent. Middle trace is an example of multiple units firing during baseline and stretch. Individual unit responses could not be determined from this sample, although all units paused during twitch contraction. The length of the muscle is shown on bottom. (**h**) Top trace, only stretch-responsive sample recorded in *Pvalb-Cre; Piezo2*^{cKO} muscle. Middle trace, representative of a non-responsive sample site. (**i**) Two representative responses to stretch from WT muscles (control littermates of *HoxB8-Cre; Piezo2*^{cKO} mice) similar to those shown in **g**. (**j**) Two stretch-responsive samples recorded in *HoxB8-Cre; Piezo2*^{cKO} muscle. For all panels, *Pvalb-Cre; Piezo2*^{cKO} mice = 4, WT mice = 3; *HoxB8-Cre; Piezo2*^{cKO} mice = 4, WT mice = 5; both EDL muscles were used for analysis except for 1 WT animal for *Pvalb-Cre*.

similar between WT and Piezo2 cKO neurons, the input resistance of Piezo2-deficient neurons was higher. Thus, less depolarizing current was required to elicit an action potential in cKO neurons (**Supplementary Table 1**). Taken together, our *in vitro* DRG recording data suggests that Piezo2 is the major mechanotransduction channel of proprioceptive neurons *in vitro*.

Piezo2 is required for MS afferent activity

To analyze proprioceptor mechanotransduction in a more physiologically relevant setting, we assayed stretch-evoked neuronal activity in WT and Piezo2 cKO mice using an *ex vivo* muscle-nerve preparation[26]. In this analysis, the extensor digitorum longus (EDL) muscle was stretched while the innervating sciatic nerve was sampled in at least two places to find stretch-induced nerve activity[26]. Muscles from all groups generated maximal tetanic forces in the healthy range[27], and no group differences in age, baseline muscle length (Lo) or contractile properties were observed between Piezo2 cKO mice and their WT controls in both strains (**Supplementary Table 2**).

Stretch-sensitive muscle afferent activity was observed in most (5 of 5 control muscles for *Pvalb-Cre*, 9 of 10 control muscles for *HoxB8-Cre*) WT muscles, whereas only one of the eight muscles for each Piezo2 cKO line exhibited any increase in afferent firing frequency during stretch (**Fig. 4a**,**b**). In WT mice, we detected at least two sample sites with stretch-sensitive activity on the nerve per muscle (5 of 5 control muscles for *Pvalb-Cre*, 7 of 10 control muscles for *HoxB8-Cre*). In Piezo2 cKO mice, we only detected one sample site from one *Pvalb-Cre; Piezo2^{cKO}* muscle and two sample sites from one *HoxB8-Cre; Piezo2^{cKO}* muscle that exhibited stretch-sensitive activity. In all WT sample sites, average firing rate following stretch increased (**Fig. 4c**,**d**), suggesting the presence of MS afferents. In contrast, no change in firing frequency during stretch occurred in most Piezo2 cKO sample sites (**Fig. 4c**,**d**). In addition, although baseline firing activity was observed in all WT sample sites (**Fig. 4c**,**d**), there was sporadic or no baseline firing activity in most Piezo2 cKO sample sites (**Fig. 4c**,**d**,**h**). This is consistent with the observation that most baseline activity in control muscles can be identified as MS afferent activity[26]. To confirm that the stretch-sensitive activity that we observed was from MS afferents, we next identified and characterized the responses of individual afferents when possible (examples of sample sites where similarities in spike shape made individual unit discrimination impossible are shown in **Fig. 4g**,**i**). All identified WT afferents displayed frequency adaptation during the hold phase of stretch, increased firing frequency in response to increasing stretch lengths (**Fig. 4e**,**f**) and paused during twitch contraction, behaviors characteristic of MS afferents[26]. The three Piezo2 cKO afferents exhibited a very small response to stretch (**Fig. 4e**,**f**,**h**,**j**), and the single *Pvalb-Cre; Piezo2^{cKO}* afferent only increased firing rate at the highest stretch length (**Fig. 4e**,**h**). In all of the muscles tested, we were able to record a group III/IV afferent response to lactic acid pH 6 administration, suggesting that the sensory deficit in Piezo2 cKO mice was limited to decreased stretch sensation (**Supplementary Fig. 7**). Collectively, our data demonstrate that the lack of Piezo2 MA channels results in a marked decrease in stretch-sensitive neuronal activity in proprioceptive muscle afferents *ex vivo*.

DISCUSSION

Mammalian proprioceptors have been characterized for nearly 50 years[10,28], yet the identity of the mechanotransduction channel underlying stretch activation in these neurons has remained unknown[4,29]. Our data show that Piezo2 is the principal MA ion channel of proprioceptors in mice. First, we found strong Piezo2 expression in MS and GTO proprioceptive sensory endings. Second, independent Piezo2-deficient mouse models revealed that proprioceptor mechanotransduction was dependent on Piezo2, as assayed by *in vitro* electrophysiological recordings of DRG neurons and an *ex vivo* muscle-nerve preparation. Finally, we observed severe proprioceptive behavioral deficits in both Piezo2-deficient strains.

Piezo2 appears to be the primary mechanosensor of proprioceptors; however, our data raise the possibility that other mechanosensor(s) exist in these neurons. Our *in vitro* DRG recording data show that some RA and IA MA currents were still present in Piezo2-deficient Pvalb$^+$ neurons. The residual RA currents can be explained by intact Piezo2 proteins from incomplete deletion by Pvalb-Cre (11.2% Pvalb$^+$ DRG neurons still retained *Piezo2* in *Pvalb-Cre*; *Piezo2^{cKO}* DRG). In contrast, IA MA currents were slightly upregulated in Piezo2-deficient neurons compared with WT neurons. This observation suggests that IA MA currents are mediated by Piezo2-independent mechanosensor(s), and that its upregulation might indicate a potential compensatory mechanism caused by Piezo2 ablation. It is, however, also possible that IA currents are more abundantly observed in Piezo2-deficient neurons because robust RA Piezo2 currents mask them in WT neurons. Notably, given that the Pvalb-Cre activity is not completely specific to proprioceptors, we do not currently know whether these Piezo2-independent IA currents are generated in Pvalb$^+$ proprioceptors or Pvalb$^+$ cutaneous mechanoreceptors[19].

There was less evidence for a second proprioceptive mechanosensitive channel from our *ex vivo* muscle-nerve recordings and behavioral analyses. In *ex vivo* muscle-nerve recordings, approximately 12% of Piezo2 cKO muscles (one of eight total muscles for both Piezo2 cKO lines) still showed stretch-activated MS-afferent firing; however, the observed stretch-sensitive responses were mostly atypical, and this could reflect the presence of residual Piezo2 (see above). At the behavioral level, there was no clear evidence for an additional mechanosensor in proprioceptors as the two lines of Piezo2 cKO mice showed full coordination defects. Taken together, our data raise the possibility that a secondary mechanotransducer channel might exist in proprioceptors; however, the identity of the channel(s) responsible for the remaining MA currents is currently unknown. Piezo1, a related mechanosensitive ion channel, is not expressed at high enough levels in sensory neurons to be a likely candidate[16], but this cannot be ruled out.

Regardless of the possibility of a second MA channel, our data suggest that Piezo2-deficient proprioceptive neurons are mostly mechanically insensitive. What happens to silenced proprioceptors with Piezo2 ablation? Anatomically, although MS-afferent endings in Piezo2 cKO muscles overall appeared to be healthy, less organized MS endings were sporadically observed, suggesting that the maintenance of MS endings might depend on the activity of proprioceptors. In addition, our *in vitro* DRG recordings revealed that the input resistance was increased in Piezo2-deficient Pvalb$^+$ neurons, whereas the resting potential and voltage threshold for action potentials were similar between WT and Piezo2-deficient neurons. Increased input resistance caused Piezo2-deficient neurons to become more excitable (that is, smaller depolarizing receptor current was needed for these neurons to fire). It is possible that a lack of mechanotransduction activity in these neurons caused the observed compensatory increase in excitability via modulating expression or function of other ion channels. A similar homeostatic change has been observed in hippocampal pyramidal neurons after complete genetic ablation of glutamatergic synaptic transmission[30]. This might represent a mechanism for the neuron to increase its gain in response to a lack of input signal.

Our *in vitro* DRG recordings showed that Piezo2-deficient proprioceptive neurons, although mechanically insensitive, were still

able to generate action potentials. These studies also revealed that MA currents mediated by proprioceptors were mainly RA. Given that MS afferents produced slowly adapting (SA) responses in response to stretch *ex vivo*, this phenomenon is reminiscent of mechanotransduction of Merkel cell-neurite complexes in the skin, where the presence of Piezo2 in both Merkel cells and sensory afferents may explain how RA transduction currents can be used to generate SA firing in sensory afferents[14,17]. How RA currents generated in proprioceptors *in vitro* convert to SA responses *in vivo* is currently unknown. It is possible that the main discrepancy is a result of the *in vitro* experimental setting, as measurements on the soma of isolated neurons may not fully recapitulate channel properties in the receptive terminals. For example, these RA currents might be modulated by accessory proteins only present in the nerve endings[29]. It is also possible that, similar to the case of Merkel cell-neurite complexes, intrafusal muscle cells express an unknown mechanosensor that modulates Piezo2 activity in MS afferents[31].

Overall, our findings elucidate a long-standing puzzle regarding the identity of the mechanotransducer of proprioceptors in mammals. Proprioception, the elusive 'sixth' sense, is crucial for coordinating the activity of motor neurons and skeletal muscles to achieve basic tasks such as standing and walking. Indeed, various diseases that affect the function of skeletal muscles, motor neurons or sensory neurons lead to profound pathological consequences. Notably, gain-of-function mutations in human PIEZO2 is associated with distal arthrogryposis type 5 (DA5)[32]. These patients develop neuromuscular and connective tissue disorders, and it has been suggested that PIEZO2 is involved in the development of joints and the neuromuscular system[32]. Although the expression of human PIEZO2 in proprioceptors and the skeletal system has not been determined, mouse Piezo2 is selectively expressed in proprioceptors and not in skeletal muscle cells. Our findings raise the possibility that DA5 could arise from dysregulated mechanotransduction in proprioceptors.

METHODS

Methods and any associated references are available in the online version of the paper.

Note: Any Supplementary Information and Source Data files are available in the online version of the paper.

ACKNOWLEDGMENTS

We thank B. Coste (Aix Marseille Université) for suggestions and H.U. Zeilhofer (University of Zurich) and R. Seal (University of Pittsburgh) for providing *HoxB8-Cre* mice. This work was supported by the Howard Hughes Medical Institute and US National Institutes of Health grant R01DE022358.

AUTHOR CONTRIBUTIONS

V.L. performed whole-cell electrophysiology in isolated DRG neurons. J.C.d.N. characterized Piezo2 cKO muscles in the laboratory of T.M.J. D.Z., C.R.C. and K.A.W. contributed to data collection and analyses for *ex vivo* muscle-nerve recordings in the laboratory of K.A.W. A.F. isolated DRG neurons for whole-cell electrophysiology. S.-H.W. contributed to all of the other experiments. S.-H.W., V.L., K.A.W. and A.P. wrote the manuscript.

COMPETING FINANCIAL INTERESTS

The authors declare no competing financial interests.

1. Sherrington, C. On the proprio-ceptive system, especially in its reflex aspect. *Brain* **29**, 467–482 (1907).
2. Proske, U. & Gandevia, S.C. The proprioceptive senses: their roles in signaling body shape, body position and movement, and muscle force. *Physiol. Rev.* **92**, 1651–1697 (2012).
3. Akay, T., Tourtellotte, W.G., Arber, S. & Jessell, T.M. Degradation of mouse locomotor pattern in the absence of proprioceptive sensory feedback. *Proc. Natl. Acad. Sci. USA* **111**, 16877–16882 (2014).
4. Bewick, G.S. & Banks, R.W. Mechanotransduction in the muscle spindle. *Pflugers Arch.* **467**, 175–190 (2015).
5. Walker, R.G., Willingham, A.T. & Zuker, C.S. A *Drosophila* mechanosensory transduction channel. *Science* **287**, 2229–2234 (2000).
6. Cheng, L.E., Song, W., Looger, L.L., Jan, L.Y. & Jan, Y.N. The role of the TRP channel NompC in *Drosophila* larval and adult locomotion. *Neuron* **67**, 373–380 (2010).
7. Tavernarakis, N., Shreffler, W., Wang, S. & Driscoll, M. unc-8, a DEG/ENaC family member, encodes a subunit of a candidate mechanically gated channel that modulates *C. elegans* locomotion. *Neuron* **18**, 107–119 (1997).
8. Li, W., Feng, Z., Sternberg, P.W. & Xu, X.Z.A. *C. elegans* stretch receptor neuron revealed by a mechanosensitive TRP channel homologue. *Nature* **440**, 684–687 (2006).
9. Suslak, T.J. *et al.* Piezo is essential for amiloride-sensitive stretch-activated mechanotransduction in larval *Drosophila* dorsal bipolar dendritic sensory neurons. *PLoS ONE* **10**, e0130969 (2015).
10. Hunt, C.C., Wilkinson, R.S. & Fukami, Y. Ionic basis of the receptor potential in primary endings of mammalian muscle spindles. *J. Gen. Physiol.* **71**, 683–698 (1978).
11. Simon, A., Shenton, F., Hunter, I., Banks, R.W. & Bewick, G.S. Amiloride-sensitive channels are a major contributor to mechanotransduction in mammalian muscle spindles. *J. Physiol. (Lond.)* **588**, 171–185 (2010).
12. Coste, B. *et al.* Piezo1 and Piezo2 are essential components of distinct mechanically activated cation channels. *Science* **330**, 55–60 (2010).
13. Li, J. *et al.* Piezo1 integration of vascular architecture with physiological force. *Nature* **515**, 279–282 (2014).
14. Maksimovic, S. *et al.* Epidermal Merkel cells are mechanosensory cells that tune mammalian touch receptors. *Nature* **509**, 617–621 (2014).
15. Ranade, S.S. *et al.* Piezo1, a mechanically activated ion channel, is required for vascular development in mice. *Proc. Natl. Acad. Sci. USA* **111**, 10347–10352 (2014).
16. Ranade, S.S. *et al.* Piezo2 is the major transducer of mechanical forces for touch sensation in mice. *Nature* **516**, 121–125 (2014).
17. Woo, S.H. *et al.* Piezo2 is required for Merkel-cell mechanotransduction. *Nature* **509**, 622–626 (2014).
18. Cahalan, S.M. *et al.* Piezo1 links mechanical forces to red blood cell volume. *eLife* **4**, e07370 (2015).
19. de Nooij, J.C., Doobar, S. & Jessell, T.M. Etv1 inactivation reveals proprioceptor subclasses that reflect the level of NT3 expression in muscle targets. *Neuron* **77**, 1055–1068 (2013).
20. McCarter, G.C., Reichling, D.B. & Levine, J.D. Mechanical transduction by rat dorsal root ganglion neurons *in vitro*. *Neurosci. Lett.* **273**, 179–182 (1999).
21. Hippenmeyer, S. *et al.* A developmental switch in the response of DRG neurons to ETS transcription factor signaling. *PLoS Biol.* **3**, e159 (2005).
22. Madisen, L. *et al.* A robust and high-throughput Cre reporting and characterization system for the whole mouse brain. *Nat. Neurosci.* **13**, 133–140 (2010).
23. Witschi, R. *et al.* Hoxb8-Cre mice: A tool for brain-sparing conditional gene deletion. *Genesis* **48**, 596–602 (2010).
24. Vrieseling, E. & Arber, S. Target-induced transcriptional control of dendritic patterning and connectivity in motor neurons by the ETS gene Pea3. *Cell* **127**, 1439–1452 (2006).
25. Arber, S., Ladle, D.R., Lin, J.H., Frank, E. & Jessell, T.M. ETS gene Er81 controls the formation of functional connections between group Ia sensory afferents and motor neurons. *Cell* **101**, 485–498 (2000).
26. Wilkinson, K.A., Kloefkorn, H.E. & Hochman, S. Characterization of muscle spindle afferents in the adult mouse using an *in vitro* muscle-nerve preparation. *PLoS ONE* **7**, e39140 (2012).
27. Brooks, S.V. & Faulkner, J.A. Contractile properties of skeletal muscles from young, adult and aged mice. *J. Physiol.* (*Lond.*) **404**, 71–82 (1988).
28. Adrian, E.D. & Zotterman, Y. The impulses produced by sensory nerve-endings. Part II. The response of a Single End-Organ. *J. Physiol.* (*Lond.*) **61**, 151–171 (1926).
29. de Nooij, J.C. *et al.* The PDZ-domain protein Whirlin facilitates mechanosensory signaling in mammalian proprioceptors. *J. Neurosci.* **35**, 3073–3084 (2015).
30. Lu, W., Bushong, E.A., Shih, T.P., Ellisman, M.H. & Nicoll, R.A. The cell-autonomous role of excitatory synaptic transmission in the regulation of neuronal structure and function. *Neuron* **78**, 433–439 (2013).
31. Zimmerman, A., Bai, L. & Ginty, D.D. The gentle touch receptors of mammalian skin. *Science* **346**, 950–954 (2014).
32. Coste, B. *et al.* Gain-of-function mutations in the mechanically activated ion channel PIEZO2 cause a subtype of Distal Arthrogryposis. *Proc. Natl. Acad. Sci. USA* **110**, 4667–4672 (2013).

ONLINE METHODS

Animals. All animal procedures were approved by The Scripps Research Institute and San José State University Institutional Animal Care and Use Committees. Animals were maintained on a 12-h light/dark cycle (lights on from 6 a.m. to 6 p.m.). Five adult animals or less were housed in one cage. Both sexes were used for all experiments except for *ex vivo* muscle-nerve recordings in which only male mice were used.

Mouse lines. *Piezo2^{GFP}-IRES-Cre* (*Piezo2^{GFP}*)[17]; *Pvalb-Cre* (The Jackson Laboratory, stock# 8069); *Piezo2$^{fl/fl}$*[17]; *HoxB8-Cre*[23]; *Ai9* (The Jackson Laboratory, stock# 7909). Note that *Pvalb-Cre; Piezo2^{cKO}* and *HoxB8-Cre; Piezo2^{cKO}* lines refer to *Pvalb-Cre; Piezo2$^{fl/-}$* and *HoxB8-Cre; Piezo2$^{fl/-}$* mice. For these Piezo2 cKO lines, *Piezo2$^{fl/+}$* mice were used as WT controls. For **Figures 2c** and **3** and **Supplementary Figures 4e** and **6**, *Pvalb-Cre; Ai9; Piezo2^{cKO}* and *Pvalb-Cre; Ai9* (WT control) mice were used to label proprioceptive neurons.

Immunofluorescence. Skeletal muscles (from hind limbs), lumbar DRG, spinal cord from the lumbar region, and dorsal skin were isolated from postnatal and adult mice, following perfusion in 4% paraformaldehyde (PFA)/phosphate-buffered saline (PBS) (wt/vol). All tissues were post-fixed in 4% PFA for 30 min to 2 h on ice and then incubated in 30% sucrose/PBS (wt/vol) overnight at 4 °C. Next day, fixed tissues were cryo-preserved in OCT and cryo-sectioned at 8 µm (for DRG and spinal cord), 20 µm (for skin) and 50–80 µm (for skeletal muscles) for immunofluorescence (IF) as previously described[17]. For IF staining, frozen sections were blocked in 10% normal goat serum (vol/vol), 1% bovine serum albumin (BSA, wt/vol) and PBS for 30 min at 25 °C. All primary antibodies were incubated in 1% BSA/PBS overnight at 4 °C. Next day, sections were incubated with secondary antibodies for 30 min at 25 °C temperature.

Antibodies. GFP (1:500, Life Technologies, A10262), Pvalb (rabbit, 1:500, Swant, PV 2; chicken, 1:10,000, ref. 19), Vglut1 (1:16,000)[33], Runx3 (1:50,000)[34], α-Bungarotoxin (1:500, Life Technologies, B13423), Piezo2 (1:1,000)[17], Nefh (1:1,000, Aves Labs, NFH).

***In situ* hybridization.** Lumbar DRG were isolated from adult mice and fixed in 4% PFA/PBS for 4 h on ice. They were then incubated in 30% sucrose/PBS overnight at 4 °C. Next day, fixed tissues were cryo-preserved in OCT and cryo-sectioned at 8 µm. Sections were subjected to *in situ* hybridization according to manufacturer's protocols (Advanced Cell Diagnostics). Bright puncta (instead of a diffuse staining pattern) represent true RNA signals.

Quantitative RT-PCR (qRT-PCR). Lumbar DRG and cervical/upper thoracic DRG from adult mice (n = 3 mice from 3 independent litters) were isolated and placed directly in TRIzol. Total RNA was isolated and subjected to qRT-PCR as previously described[16,17].

DRG cultures and whole-cell electrophysiology. DRG from 4–6-week-old *Pvalb-Cre; Ai9* (WT control) and *Pvalb-Cre; Ai9; Piezo2^{cKO}* mice were isolated and dissociated for neuronal cultures as previously described[12]. All DRG neurons including both tdTomato$^+$ and tdTomato$^-$ neurons were plated together onto poly-D-lysine– and laminin-coated coverslips (day 0). DRG neurons were cultured at least overnight and were used for patch-clamp recording experiments from days 1–3.

Patch-clamp experiments were performed in standard whole-cell configuration using an Axopatch 200B amplifier (Axon Instruments). Patch pipettes were pulled to a resistance of 2–4 MΩ using a Flaming-Brown P97 pipette puller (Sutter Instruments). Pipette solutions for I-V measurements consisted of (in mM) 90 cesium gluconate, 10 CsCl, 10 HEPES, 5 EGTA, 1 $CaCl_2$, 5 $MgCl_2$, 4 Na_2ATP, and 0.4 Na_2GTP (pH adjusted to 7.3 with CsOH). The extracellular solution for I-V measurements consisted of (in mM): 40 TEA-Cl, 100 NaCl, 4 KCl, 1.25 $CaCl_2$, 1 $MgCl_2$, 10 HEPES, 10 glucose (pH adjusted to 7.3 with NaOH). All other measurements were conducted using a pipette solution consisting of (in mM): 125 potassium gluconate, 7 KCl, 1 $CaCl_2$, 5 $MgCl_2$, 10 HEPES, 1 EGTA, 4 Na_2ATP, and 0.4 Na_2GTP (pH adjusted to 7.3 with CsOH) and an extracellular solution consisting of (in mM): 137 NaCl, 4 KCl, 1.25 $CaCl_2$, 1 $MgCl_2$, 10 HEPES, 10 glucose (pH adjusted to 7.4 with NaOH). All experiments were conducted at 25 °C. Currents were sampled at 5 kHz and filtered at 2 kHz. Mechanical stimulation of DRG cell bodies was achieved as described previously[12]. For I-V recordings, neurons were held at 0 mV and stepped to test voltages for duration of 4 s to allow for a steady state in residual voltage-activated currents. The mechanical stimulus was applied at the end of the 4 s interval. Background currents before mechanical stimuli were subtracted offline from recorded traces.

Muscle spindle afferent recordings from isolated muscle nerve preparation. Muscle sensory neuron response to physiological stretch was assayed *ex vivo* using an isolated muscle-nerve preparation as previously described[26]. Briefly, the extensor digitorum longus (EDL) muscle and deep peroneal branch of the sciatic nerve were placed in an oxygenated tissue bath. The tendons were sutured to a tissue post and a lever arm connected to a dual force and length controller and transducer (300C-LR, Aurora Scientific). Baseline muscle length was set at the length at which maximal twitch contractile force was generated (Lo). A suction electrode (tip diameter 50–100 µm) connected to an extracellular amplifier (Model 1800, A&M Systems) was used to sample sensory activity. The nerve was sampled to find stretch sensitive sensory activity and a series of 9 ramp and hold stretches was given (3 stretches each to Lo plus 2.5%, 5% and 7.5% Lo; ramp speed 40% Lo s^{-1}; stretches held 4 s with 1 min in between each stretch). Sensory response to a series of 60 twitch contractions given at 1-Hz frequency was then sampled to look for a characteristic pause in muscle spindle afferent firing during contraction[35]. If no stretch sensitive activity was found, the response to stretch at 2–3 unique electrode placements on the nerve was still recorded to ensure that stretch sensitive activity did not appear following repeated stretch. Sensory response to a 10-min exposure to a 15 mM lactic acid (pH 6) solution was also measured to ensure that the sensory deficit was specific to stretch. Muscle health was determined by comparing the maximal contractile force during a tetanic stimulation (500-ms train, 120-Hz frequency, 0.5-ms pulse width, supramaximal voltage) to previously reported values[27]. The number of muscles in which stretch sensitive activity could be recorded was determined for each group. For each electrode placement, we quantified the average baseline firing rate and the static stretch response (firing rate during the plateau phase of stretch (3.25–3.75 s into the stretch; see **Fig. 4g**) – baseline firing rate). Individual sensory neurons were identified by spike shape when possible by using the Spike Histogram feature of Lab Chart (AD Instruments; **Fig. 4g**). An individual neuron was classified as a putative muscle spindle afferent if it displayed a characteristic instantaneous frequency response to stretch as well as a pause during twitch contraction[35]. Spindle afferent baseline firing rate and static stretch response were then determined as described above[26].

Sample size and randomization. For *ex vivo* muscle spindle afferent recordings: *Pvalb-Cre; Piezo2^{cKO}* mice = 4 from 2 independent litters and WT mice = 3 from 3 litters; *HoxB8-Cre; Piezo2^{cKO}* mice = 4 from 3 litters and WT mice = 5 from 3 litters. For all other experiments (except in **Supplementary Fig. 5**: 3 mice from 3 independent litters were used for qRT-PCR and *in situ* hybridization), at least 4 mice from at least 4 independent litters per genotype were used. Immunofluorescent staining yielded consistent results for every experiment, so our current sample size is sufficient. *In vitro* DRG recordings and *ex vivo* muscle-nerve recordings mostly yielded all or none responses for all recording experiments; therefore, our current sample size is justified. All experiments were repeated at least three times. All animals were randomly selected for experiments. Immunofluorescent studies were performed in a blind manner. Conditional knockout mouse characterization could not be performed in a blind manner due to behavioral conditions observed in *Piezo2* conditional knockout mice.

A **Supplementary Methods Checklist** is available.

33. Demireva, E.Y., Shapiro, L.S., Jessell, T.M. & Zampieri, N. Motor neuron position and topographic order imposed by beta- and gamma-catenin activities. *Cell* **147**, 641–652 (2011).
34. Kramer, I. *et al.* A role for Runx transcription factor signaling in dorsal root ganglion sensory neuron diversification. *Neuron* **49**, 379–393 (2006).
35. Hunt, C.C. & Kuffler, S.W. Stretch receptor discharges during muscle contraction. *J. Physiol. (Lond.)* **113**, 298–315 (1951).